2-2009

Shear Banding Or Not in Entangled Dna Solutions Depending on the Level of Entanglement

Pouyan E. Boukany
University of Akron Main Campus

Shi-Qing Wang
University of Akron Main Campus, swang@uakron.edu

Shear banding or not in entangled DNA solutions depending on the level of entanglement

Pouyan E. Boukany and Shi-Qing Wang[a)]

Department of Polymer Science, University of Akron, Akron, Ohio 44325

(Received 28 November 2007; final revision received 6 October 2008)

Synopsis

Entangled DNA solutions are ideal as a model system to examine nonlinear shear flow behavior. Even when the number of entanglements per chain, Z, is higher than 100, the solution is still soft enough with an elastic plateau modulus under 100 Pa and is thus amenable to experimental study by commercial rotational rheometry without ambiguity and uncertainty. We have investigated nonlinear flow behavior of three entangled DNA solutions with $Z=24$, 60, and 156, respectively, using a combination of particle-tracking velocimetric (PTV) and conventional rheometric measurements. We explore questions such as (a) whether shear banding also occurs in moderately entangled solutions, (b) whether creep results in development of nonlinear velocity profile, (c) whether shear banding produced in startup shear and creep persists at long times in steady state, and (d) whether these entangled solutions exhibit homogeneous shear at the upper end of the stress plateau region. We found that the first DNA solution ($Z=24$) only shows transient weakly inhomogeneous shear and steady linear velocity profile. In the more entangled solutions ($Z=60$ and 156), shear banding is observed in startup rate- and stress-controlled shear in the shear thinning regime. Shear homogeneity eventually returns at the upper end of the stress plateau (shear thinning) regime. © *2009 The Society of Rheology.* [DOI: 10.1122/1.3009299]

I. INTRODUCTION

A conventional way to investigate flow behavior of complex fluids is to employ a rotational rheometer to measure the generated shear stress as a function of time for a given rate of shear. Stress overshoot shows up in such a rheometric setup during startup shear of entangled polymer solutions when the Weissenberg number Wi is appreciably higher than unity [Huppler *et al.* (1967); Menezes and Graessley (1982); Osaki *et al.* (2000a, 2000b); Pattamaprom and Larson (2001); Tapadia and Wang (2004)]. If steady state can be achieved, one obtains a flow curve of shear stress versus averaged shear rate. Typically, such a flow curve is smooth and shows stress plateau beyond the Newtonian regime for monodisperse entangled polymers. The latest theoretical description [Graham *et al.* (2003)] also anticipated smooth monotonic constitutive relationship. Existence of monotonic flow curves have led to the suggestion [Graham *et al.* (2003); Hu *et al.* (2007)] that there would not be inhomogeneous shear of entangled polymers in steady state in a simple-shear apparatus.

The signature of stress plateau in a flow curve invited us to examine the rheological behavior of entangled polymer solutions in creep mode [Tapadia and Wang (2004);

[a)]Author to whom correspondence should be addressed; electronic mail: swang@uakron.edu

Ravindranath and Wang (2008)]. One elusive question is whether an entangled polymer can possess different states of entanglement corresponding to the same shear stress during startup shear. Recent particle-tracking-velocimetric (PTV) studies from different groups reported that shear banding at least occur transiently [Tapadia and Wang (2006); Boukany and Wang (2007); Hu *et al.* (2007)].

In this work, we choose DNA solutions to model entangled polymer systems. A previous study by Ravindranath and Wang (2008) on polymer solutions has shown that moderately concentrated solutions do not suffer from edge instability that requires special care to avoid its rheological consequence. At concentrations as low as anywhere between 5 and 22 mg/mL for the DNA solution, edge fracture should also be negligible. Consequently, we can conveniently study steady-state flow behavior during startup flow in both rate- and stress-controlled modes as a function of chain entanglement ranging from $Z = 24$ to 156, where Z is the estimated number of entanglements per chain. Based on our PTV setup, we show that at $Z = 24$ only transient shear banding is observed beyond the stress overshoot. In the other two solutions with $Z = 60$ and 156, shear inhomogeneity is observed to persist in steady state in both rate-controlled and stress-controlled startup modes.

II. EXPERIMENT

A. Materials

In this study, we use linear double-strand DNA calf thymus as a model system. The highly purified DNA with a weight-average molecular weight of 50×10^6 (g/mol) or 7.5×104 base pairs (bp) was purchased from USB Co. Our three DNA solutions involve glycerol (Fluka, Catalog No. 49767) as the solvent. All samples were prepared by dissolving both DNA and glycerol in a buffer containing 10 mM Tris-HCl (*p*H 7.9) to obtain uniform molecular mixing. Specifically, the three concentrations at 5, 11, and 22 mg/mL of DNA were, respectively, mixed in a buffer with 5, 10, and 20 mM of NaCl and 0.2, 0.4, and 0.8 mM of ethylene diamine tetraacetic acid. Then, the water was allowed to evaporate for several days. The final sample has about 1%–2% residual water. To inhibit degradation, the DNA solution was stored in refrigerator at $T \sim 4\ ^\circ$C after mixing. About 300–500 ppm of silver-coated particles (Dantec Dynamic HGS-10, which as a size range from 1 to 20 μm) were uniformly dispersed in the DNA solution for tracking the velocity profile. The basic structural information and other literature background have been provided for a water-based solution [Boukany *et al.* (2008)]. We expect similar characteristics associated with the current solutions, in terms of DNA coil size and level of entanglement, judging from their linear viscoelastic properties [Boukany and Wang (2008)].

B. Methods of PTV and rheometry

Rheological and PTV measurements were carried out using a Physica MCR-301 rotational rheometer (Anton Paar) in a cone-plate setup, all at room temperature around 23 °C. For conventional rheometric measurements, a cone of angle 2° and diameter 25 mm is employed. To enable PTV observations, a sheet of laser passes across the sample thickness, and a charge coupled device camera captures movements of the illuminated particles onto a VCR. To observe the flow field inside the sample, a flexible transparent film with diameter around 27 mm is wrapped around the meniscus of a cone-plate assembly with 4° cone angle and 25 mm diameter. The PTV observation plane is 3–4 mm from the meniscus. A schematic drawing can be found elsewhere [Boukany and Wang (2008)].

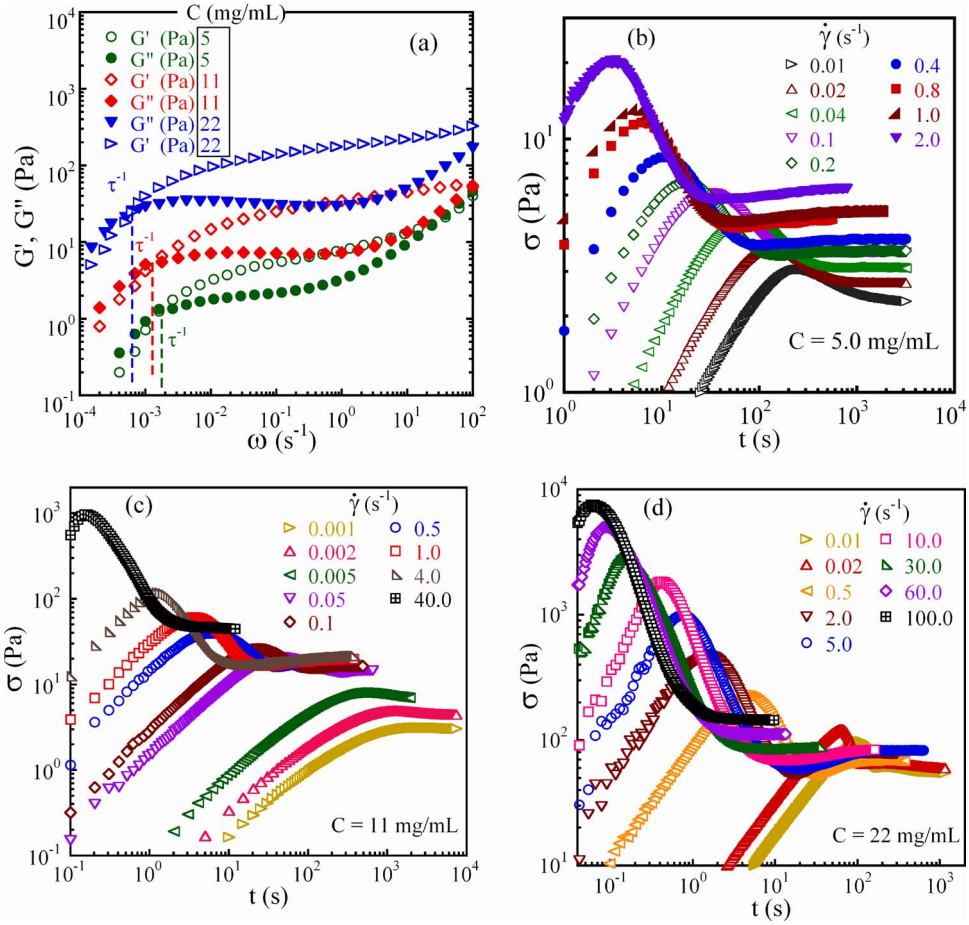

FIG. 1. (a) Storage G' and loss moduli versus a frequency for the three solutions (Z=24, 60, and 156). (b)–(d) Time-dependent shear stress σ (Pa) during startup shear at different imposed shear rates.

III. RESULTS AND DISCUSSSION

A. Linear and nonlinear rheometric measurements

Storage and loss moduli G' and G'' versus frequency ω three concentrations of C =5.0, 11, and 22 mg/mL have been obtained from small amplitude oscillatory shear measurements as shown in Fig. 1(a). The characteristics of these samples based on the SAOS measurements are listed Table I, where the plateau modulus G_p was estimated from the value of G' at the frequency, where G'' shows a minimum, and the terminal

TABLE I. Characteristics properties of DNA solutions.

C (mg/mL)	G_p (Pa)	M_e (C) (g/mol)	$Z(C)=M_w/M_e(C)$	τ (s)	$\tau_R=\tau/3Z$ (s)	$a_L=[6R_g^2/Z(C)]^{1/2}$ (μm)	η_{bulk} (Pa s)	$b_{max}=(\eta_{bulk}/\eta_i)a_L$ (mm)
5.0	5.83	2.1×10^6	24	550	7.6	0.325	900	0.4
11.0	32	0.84×10^6	60	780	4.3	0.205	7800	2.13
22.0	169	0.32×10^6	156	1590	3.4	0.127	58450	9.9

relaxation time τ is taken as the inverse of the crossover frequency where $G'=G''$. The critical entanglement molecular weight $M_e(C)$ is estimated from $M_e(C)=CRT/G_p(C)$, where C, R, T are the concentration, gas constant, and temperature, respectively. Number of entanglements per chain is estimated by $Z(C)=M_w/M_e(C)$. The tube diameter a_L of these DNA solutions is estimated from $a_L^2=6R_g^2/Z(C)$, where the coil size $R_g=2l_p(aN/12l_p)^{\upsilon}$ is estimated according to Mason *et al.* (1998) with $a=0.34$ nm being the length of base pair, $N=7.5\times10^4$ bp, the persistence length $l_p\sim0.050$ μm, and $\nu=0.5$ for a θ solvent. The slip length b of these sample can be calculated according to $b=(\eta_{\text{bulk}}/\eta_i)a_L$ [Ravindranath and Wang (2007)] where η_{bulk} is taken as the zero-shear viscosity and $\eta_i\sim0.75$ Pa s is taken as the viscosity of the solvent, i.e., that of glycerol.

Figures 1(b)–1(d) display the growth of shear stress (Pa) as a function of time at various imposed averaged shear rates for $C=5$, 11, and 22 mg/mL, respectively. At low shear rates when $\dot{\gamma}_{\text{app}}<\tau^{-1}$, the stress growth is monotonic. Stress overshoot occurs at higher shear rates in the stress plateau regime when $\dot{\gamma}_{\text{app}}>\tau^{-1}$. More stress overshoot behavior is presented in supplemental material (See Supplementary Material in EPAPS document E-JORHD2-53-007901. Information on accessing this document is contained at the end of the paper.) where we also present systematic creep tests for these solutions where the apparent rate rises with time at each applied stress, and three flow curves for these three solutions, obtained with oscillatory shear, startup rate-controlled, and stress-controlled shear, respectively.

B. PTV measurements

It is important to find out whether entangled solutions would always suffer flow inhomogeneity upon startup shear in the nonlinear regime where stress overshoot is a common characteristic. PTV measurements have recently shown to provide some insight into the origins of various rheological responses. The present study applies the PTV method to determine whether shear banding is permanent in systems ranging from moderately entangled to highly entangled samples.

1. Homogeneous shear for less entangled solutions ($Z\sim24$)

Figures 2(a) and 2(b) show the transient behavior of 5 mg/mL DNA/glycerol solution ($Z=24$) at $\dot{\gamma}_{\text{app}}=0.2$, and 1.0 s^{-1} respectively: the velocity profile is linear until the stress maximum; after the stress maximum, weak inhomogeneous shear appeared across the gap during the sharp stress decline. However, at long times the velocity profile returned to linearity. Figures 3(a) and 3(b) show the steady-state velocity profiles at different shear rates from 0.01 to 2.0 s^{-1} that are approximately linear.

2. Permanent shear banding at highly entangled solutions ($Z>60$)

a. Slip-like behavior at lower shear rates. At a low shear rate $\dot{\gamma}_{\text{app}}=0.05$ s^{-1}, the velocity profile of the second solution of $Z=60$ is linear before the stress overshoot and shows apparent wall slip after the stress maximum as shown in Figs. 4(a) and 4(b). Limited by the spatial resolution (around 20 μm) of the current PTV method, we cannot discern the thickness of the thin high shear band. On the other hand, the PTV technique was perfectly adequate to reveal that the bulk of the sample experiences a shear rate of 0.013 s^{-1} that is ten times the reciprocal of the terminal relaxation time ($\tau=780$ s). This is consistent with the data in Fig. 1(c) that the steady shear stress is noticeably higher at 0.05 s^{-1} than that at 0.001 or 0.002 s^{-1}.

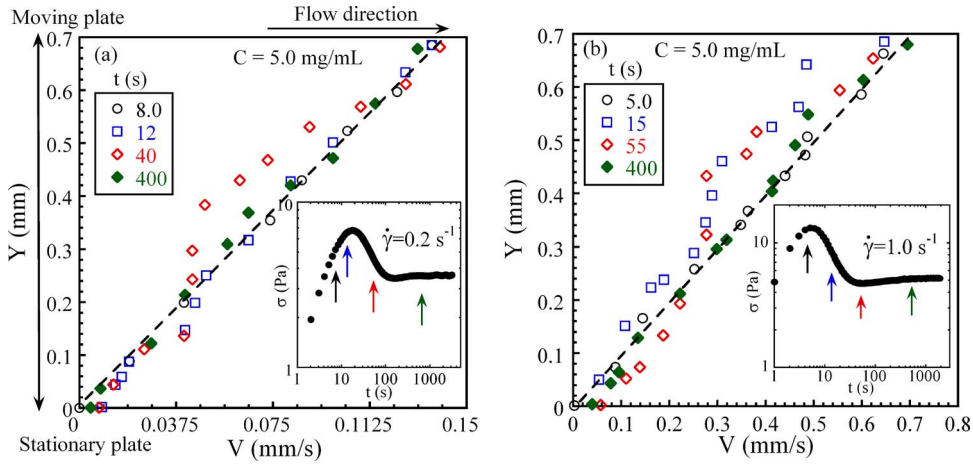

FIG. 2. PTV measurements of velocity profile at different times during startup shear with (a) $\dot{\gamma}_{app}$=0.2 s^{-1} and (b) $\dot{\gamma}_{app}$=1.0 s^{-1}, for the least entangled solution of C=5.0 mg/mL (Z=24) where the insets show the time-dependent stress growth.

b. Startup shear: Transient and steady state banding. Because of plausibly few entanglements at the sample/wall interface, shear inhomogeneity first occurs in the form of wall slip when the applied rate is higher than the overall relaxation rate. For a higher rate, the bulk of the sample has to develop a region of high shear in response. This region may be too thin for our PTV measurements to determine, as shown to be the case in the preceding paragraph for $\dot{\gamma}_{app}$=0.05 s^{-1}. At a higher shear rate $\dot{\gamma}_{app}$=0.5 s^{-1}, after the stress maximum at t=15 s, shear banding developed across the gap as shown in Figs. 5(a) and 5(b). In other words, for this rate, a high-shear band of measurable thickness emerges. After a stress minimum (undershoot) at t>50 s, the shear banding persisted across the gap, and stress signal reached steady state at t=200 s. In addition to presence of a high-shear band of measurable thickness, the bulk also suffers a shear rate around 0.036 s^{-1} that is significantly higher than the terminal relaxation rate τ^{-1}. In other words, during this shear

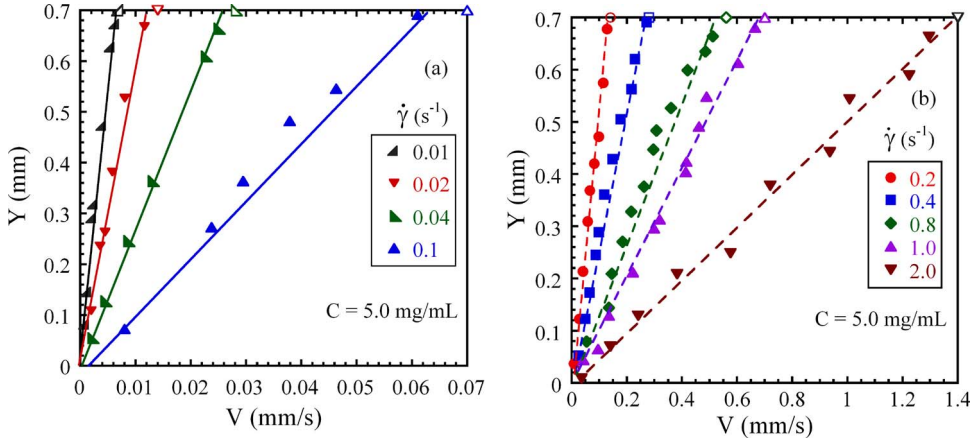

FIG. 3. The steady-state velocity profiles from PTV measurements at various applied rates (a) from $\dot{\gamma}_{app}$ =0.01 to 0.1 s^{-1}, (b) from $\dot{\gamma}_{app}$=0.2 to 2.0 s^{-1}. Open symbols represent the imposed velocity on the top moving plate.

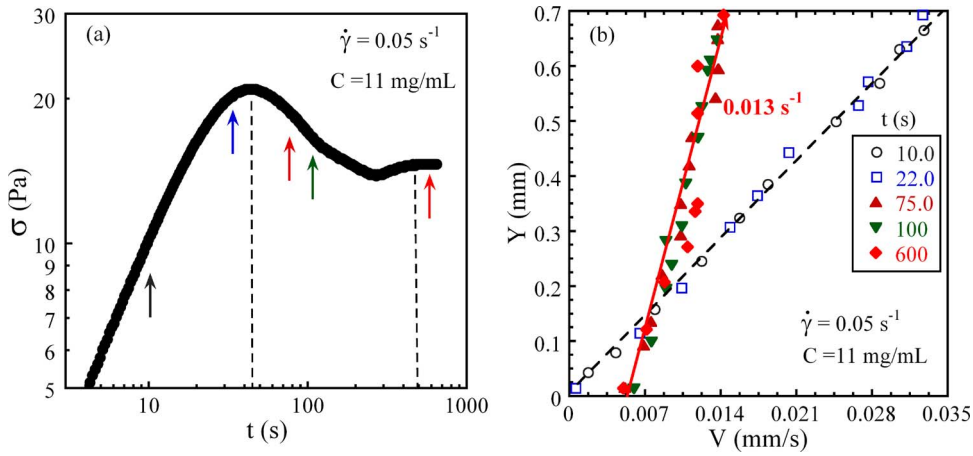

FIG. 4. (a) Time-dependent shear stress at $\dot{\gamma}_{app}$=0.05 s^{-1}. (b) The corresponding velocity profile at different times, for the solution of C=11.0 mg/mL (Z=60).

banding in steady state, the bulk of the sample is undergoing shear significantly faster than terminal flow. At an even higher rate of 2 s^{-1}, Figs. 6(a) and 6(b) further confirm that permanent banding remain in steady state after 700 strain units and the bulk shear rate increases further to 0.13 s, which 100 times higher the terminal relaxation rate of 1/780 s^{-1}. The thickness of high-shear band grows with increasing shear rates from 0.5 to 2.0 s^{-1}. Corresponding to the steady state depicted in Fig. 6(b), we provide one video clip in the supplemental material to show how the velocity profile looks in a real-time movie based on our PTV technique (see supplementary material in EPAPS document E-JORHD2-53-007901).

c. Rupture-like recoil and steady state banding for a most entangled solution. Figures 7(a) and 7(b) reveal the transient behavior of the third DNA solution (Z=156) at $\dot{\gamma}_{app}$ =0.5 s^{-1}. The velocity profile is linear till the stress maximum. After the stress maximum,

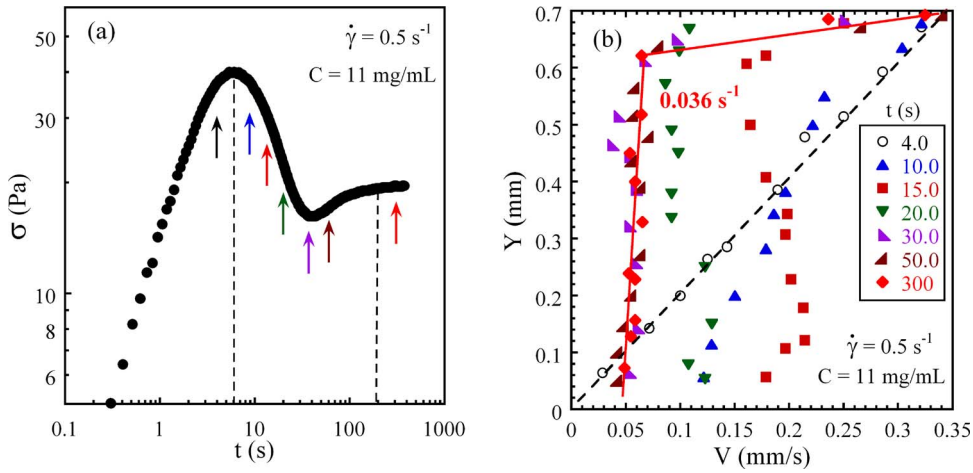

FIG. 5. (a) Time-dependent shear stress at $\dot{\gamma}_{app}$=0.5 s^{-1}. (b) The corresponding velocity profile at different times, for the solution of C=11.0 mg/mL (Z=60).

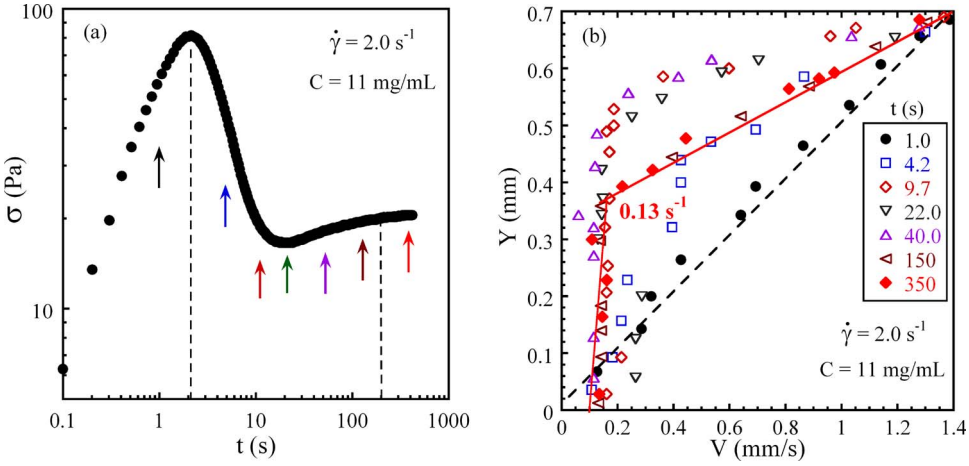

FIG. 6. (a) Time-dependent shear stress at $\dot{\gamma}_{app}$=2.0 s^{-1}. (b) The corresponding velocity profile at different times, for the solution of C=11.0 mg/mL (Z=60).

the velocity profile changed dramatically. At t=10.5 s, the local velocity in part of the sample attained a negative value reflecting recoil upon cohesive breakdown. After a stress minimum at t=20 s, the recoil was over. At t=100 s, the stress reached a steady state and permanent banding remained across the gap. Once again the bulk shear rate of 0.077 s^{-1} is much higher than the terminal relaxation rate of τ^{-1}=0.00063 s^{-1}, indicating the low-shear band is not undergoing terminal flow at all. At a higher shear rates $\dot{\gamma}_{app}$=5.0 s^{-1}, the transient recoil-like response with a negative slope no longer occurs as shown in Figs. 8(a) and 8(b). Shear banding still persisted after 1000 strain units (t=200 s).

d. Creep mode. In this section, we imposed external deformation at various fixed shear stresses either below or comparable to the level seen in the stress plateau region. Figure 9 shows that at a low shear stress of σ=15 Pa, the second DNA solution (Z=60) suffered considerable apparent wall slip in steady state that reached an apparent shear rate of 0.03 s^{-1}, with a velocity profile completely similar to Fig. 4(b) obtained in the rate-

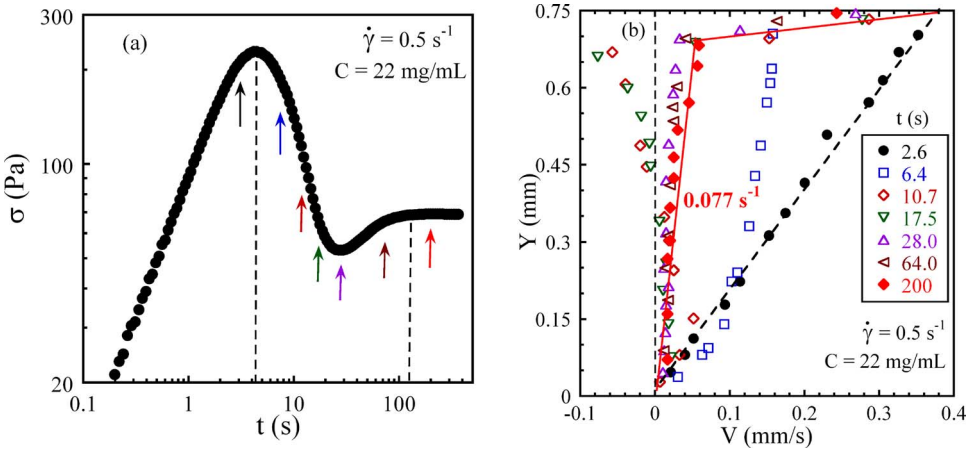

FIG. 7. (a) Time-dependent shear stress at $\dot{\gamma}_{app}$=0.5 s^{-1}. (b) The corresponding velocity profile at different times, for the solution of C=22.0 mg/mL (Z=156).

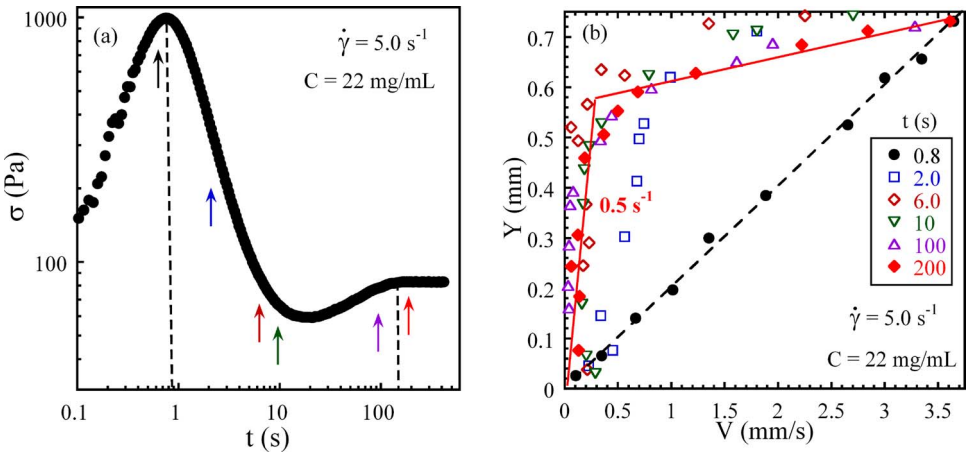

FIG. 8. (a) Time-dependent shear stress at $\dot{\gamma}_{app}$=5.0 s^{-1}. (b) The corresponding velocity profile at different times, for the solution of C=22.0 mg/mL (Z=156).

controlled mode at 0.05 s^{-1}. At a higher shear stress of σ=21 Pa as shown in the same figure, permanent shear banding was observed across the gap, attaining a final apparent rate of 1.4 s^{-1}. The velocity profile resembles Figs. 5(b) and 6(b). Similar creep results were obtained in the third solution of Z=156, confirming that the startup creep is unable to produce homogeneous shear in the well entangled solutions. This is an important conclusion, consistent with the recent findings in polymer solutions [Ravindranath and Wang (2008)].

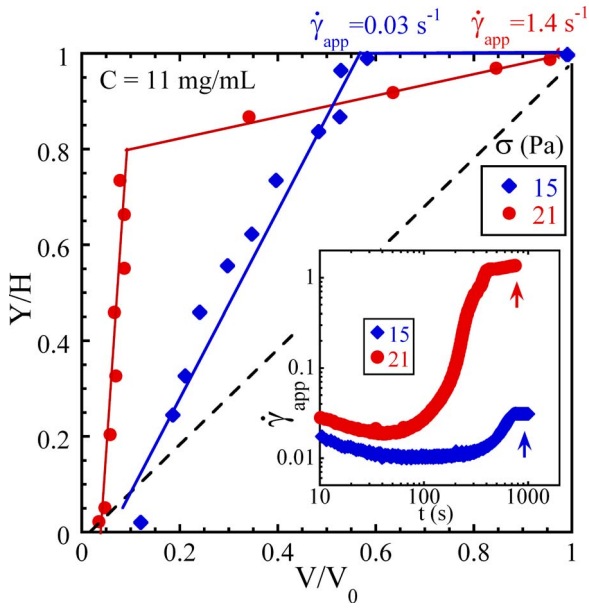

FIG. 9. Normalized steady state velocity profiles during creep at 15 and 21 Pa, respectively, for the solution of C=11.0 mg/mL (Z=60); where H is the gap distance and V_0 is the velocity of the moving surface so that by definition $\dot{\gamma}_{app}=V_0/H$. The inset shows increase of $\dot{\gamma}_{app}$ as a function of time.

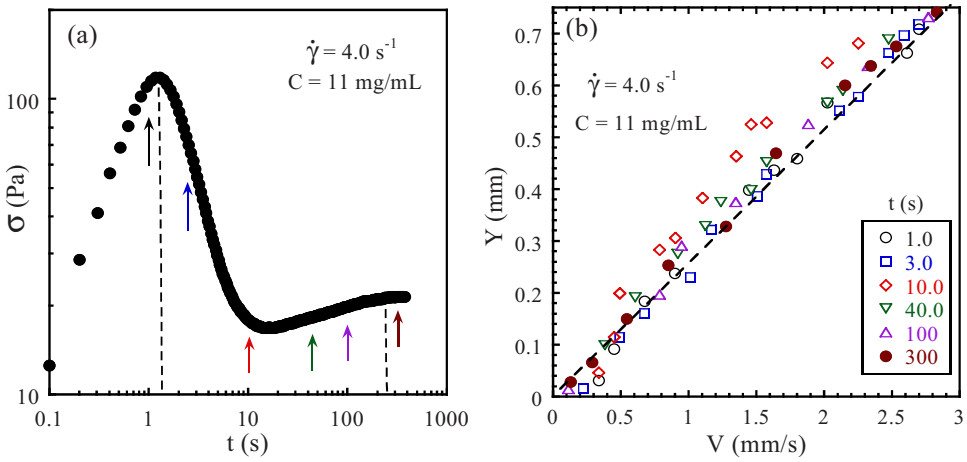

FIG. 10. (a) Time-dependent shear stress at $\dot{\gamma}_{app}$=4.0 s^{-1} (near the end of the stress plateau). (b) The corresponding almost linear velocity profile at different times, for the solution of C=11.0 mg/mL (Z=60).

3. Recovery of homogenous shear at upper end of plateau region

a. Startup (rate-control mode). At average shear rates close to the upper end of the stress plateau region, the velocity profile returned to linearity as shown in Fig. 10 for $\dot{\gamma}_{app}$=4.0 s^{-1} in the second solution (Z=60). At t=10 s, weak inhomogeneous flow was observed across the gap. However, at longer times (steady state), the velocity profile is fairly linear across the sample thickness. Figures 11(a) and 11(b) summarize for both solutions the progressive development from shear banding to shear homogeneity as the applied rate swept across the stress plateau.

b. Creep (stress-control mode). In creep at a higher shear stress of σ=22 Pa, the apparent shear rates gradually rises as a function of time as shown in Fig. 12(a), where the

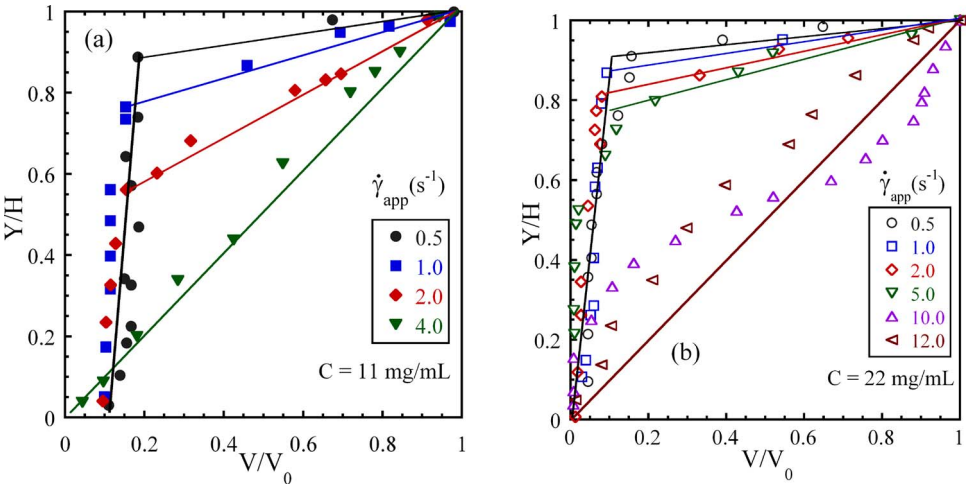

FIG. 11. Normalized steady-state velocity profiles at various rates for (a) the solution at C=11.0 mg/mL, where $\dot{\gamma}_{app}$ is between 0.05 and 4.0 s^{-1}, and for (b) the solution at C=22.0 mg/mL, where $\dot{\gamma}_{app}$ is between 0.1 and 12.0 s^{-1}.

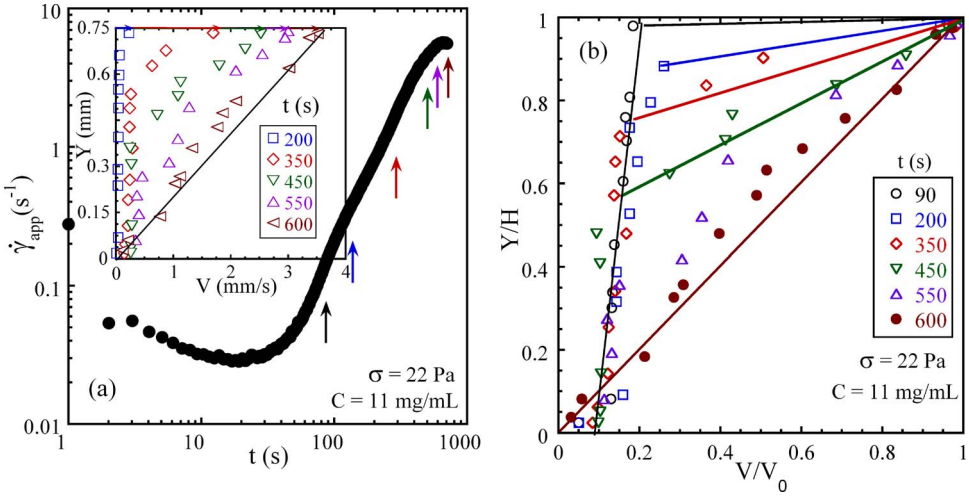

FIG. 12. (a) Rise of the apparent rate with time during creep at a higher stress of 22 Pa for the solution with C=11.0 mg/mL, where the inset shows the PTV measurements of time evolution of the actual velocity profile. (b) The normalized velocity profiles, where H is the gap distance and V_0 is the velocity of the moving surface, to show how the system transforms from initial apparent wall slip to the eventual shear homogeneity.

inset shows the corresponding PTV measurements of the velocity profile. At t=90 s, there was only wall slip as shown in Fig. 12(b). A thin layer of high-shear developed from the top surface at t=200 s. As the apparent shear rate rose further, the thickness of high-shear band grew. Finally, at t=600 s, the shear rate reaches a steady-state value around 4.8 s^{-1}, and the velocity profile was nearly linear. Apparently, creep at a higher stress also recovers homogeneous shear, when it produces a shear rate higher than 4.0 s^{-1}, at which rate-controlled startup shear also generated a linear velocity profile as shown in Fig. 10(b).

IV. SUMMARY

We have studied nonlinear flow behavior of the entangled DNA solutions with different levels of entanglement from Z=24 to 156. In the relatively less entangled solution (Z=24), weakly inhomogeneous shear was transiently observed after stress overshoot in startup shear. However, the steady state velocity profile is linear. In the other two solutions (Z=60, 156, respectively), permanent shear banding was unambiguously observed in the sample interior upon startup shear in both rate- and stress-controlled modes in the stress plateau regime. In both modes immediate rates beyond the terminal regime produces apparent wall slip. At high rates, shear inhomogeneity occurs in the form of bulk shear banding. Near the upper end of the stress plateau, homogeneous shear reemerges at long times in both modes of shear.

ACKNOWLEDGMENTS

This work is supported, in part, by a small grant for exploratory research (DMR-0603951) and a regular grant (DMR-0821697) from National Science Foundation.

References

Boukany, P. E., and S. Q. Wang, "A correlation between velocity profile and molecular weight distribution in sheared entangled polymer solutions," J. Rheol. **51**, 217–233 (2007).

Boukany, P. E., and S. Q. Wang, "Exploring the transition from wall slip to bulk shearing banding in well-entangled DNA solutions," Soft Matter (2008) (in press).

Boukany, P. E., Y. T. Hu, and S. Q. Wang, "Observations of wall slip and shear banding in an entangled DNA Solution," Macromolecules **41**, 2644 (2008). Many references can be found here regarding the relevant literature on rheology and single-chain visualization studies of DNA solutions.

Graham, R. S., A. E. Likhtman, and T. C. B. McLeish, "Microscopic theory of linear, entangled polymer chains under rapid deformation including chain stretch and convective constraint release," J. Rheol. **47**, 1171–1200 (2003).

Hu, Y. T., L. Wilen, A. Philips, and A. Lips, "Is the constitutive relation for entangled polymers monotonic?," J. Rheol. **51**, 275–295 (2007).

Huppler, J. D., I. F. Macdonal, E. Ashare, T. W. Spriggs, and R. B. Bird, "Rheological properties of three solutions. Part II. Relaxation and growth of shear and normal stresses," Trans. Soc. Rheol. **11**, 181–204 (1967).

Mason, T. G., A. Dhople, and D. Wirtz, "Linear viscoelastic moduli of concentrated DNA solutions," Macromolecules **31**, 3600 (1998).

Menezes, E. V., and W. W. Graessley, "Non-linear rheological behavior of polymer systems for several shear-flow histories," J. Polym. Sci., Part A-2 **20**, 1817–1833 (1982).

Osaki, K., T. Inoue, and T. Uematsu, "Stress overshoot of polymer solutions at high rates of shear: Semi-dilute polystyrene solutions with and without chain entanglement," J. Polym. Sci., Part B: Polym. Phys. **38**, 3271–3276 (2000a).

Osaki, K., T. Inoue, and T. Isomura, "Stress overshoot of polymer solutions at high rates of shear," J. Polym. Sci., Part B: Polym. Phys. **38**, 1917–1925 (2000b).

Pattamaprom, C., and R. G. Larson, "Constraint release effects in monodiesperse and bidisperse polystyrenes in fast transient shearing flows," Macromolecules **34**, 5229–5237 (2001).

Ravindranath, S., and S. Q. Wang, "Steady state measurements in stress plateau region ofentangled polymer solutions: Controlled-rate and controlled stress modes," J. Rheol. **52**, 957–980 (2008).

See EPAPS Document No. E-JORHD2-53-007901 for additional figures and a real-time video showing shear banding in steady state. For more information on EPAPS, see http://www.aip.org/pubservs/epaps.html.

Tapadia, P., and S. Q. Wang, "Nonlinear flow behavior of entangled polymer solutions:yieldlike entanglement-disentanglement transition," Macromolecules **37**, 9083–9095 (2004).

Tapadia, P., and S. Q. Wang, "Direct visualization of continuous simple shear in non-Newtonian polymeric fluids," Phys. Rev. Lett. **96**, 016001 (2006).